



Trade Science Inc.

Materials Science

An Indian Journal

Full Paper

MSAIJ, 5(4), 2009 [289-298]

Electrodeposition of bright Zn-Fe alloy on mild steel from acid chloride bath

K.Venkatakrishna¹, A.Chitharanjan Hegde^{*1}, N.Eliaz²¹Department of Chemistry, National Institute of Technology Karnataka, Srinivasnagar- 575 025, (INDIA)²Biomaterials and Corrosion Laboratory, Tel-Aviv University, Ramat-Aviv 69978, (ISRAEL)

E-mail : achegde@rediffmail.com

Received: 24th June, 2009 ; Accepted: 4th July, 2009

ABSTRACT

Electrodeposition of Zn-Fe alloy on mild steel substrate was performed under galvanostatic condition from an acid chloride bath. Use of sulphanic acid (SA) and gelatin was found to show significant effect on homogeneity and brightness of the deposit. Under no conditions of bath composition and operating parameters studied, the codeposition behaviour changed from anomalous to normal type was observed. The experimental results revealed that the corrosion resistance of electroplates depends on both wt. % Fe and structure of the deposit. The dependency of bath composition, current density (c.d.), pH and temperature on wt % of Fe, hardness, appearance and corrosion resistance of deposits were studied and discussed. The corrosion resistance of electroplates were evaluated by direct current (d. c.) and alternate current (a. c.) method. Potentiodynamic cyclic polarisation technique was used to investigate the mechanism of corrosion. The surface roughness and morphology of deposits were studied by AFM and SEM analysis. XPS analysis was carried out to investigate the state of metal in the alloy. The electrochemical impedance spectroscopy (EIS) analysis revealed that superior corrosion resistance of Zn-Fe coatings are due to formation of n-type semiconductor film at the interface of the metal and medium, confirmed by Mott-Schottky (M-S) plot. © 2009 Trade Science Inc. - INDIA

KEYWORDS

Zn-Fe alloy;
Chloride bath;
Sulphanilic acid and
gelatin.

INTRODUCTION

Codeposition of two metals requires that their individual reversible potentials are reasonably close to each other in the specific bath. This is the case when their standard potentials are close, when the concentration of one of the metals in solution is properly tuned, or when complexing agent that forms complexes with different stability constants is added. Among the variety

of electrodeposition, the deposition of Zn-M (where M = Ni, Co and Fe) is of great interest because of their high corrosion resistance compared to that of pure zinc^[1-3]. It has been shown that the corrosion potential of the electrodeposited Zn-Fe alloy is 10% nobler and corrosion current is two times smaller than those of pure zinc coating of equal thickness^[4-6]. Improvements in corrosion resistance of Zn-M alloys are believed due to introduction of slightly nobler metal into the crystal

Full Paper

lattice. Therefore many studies have been attempted to understand the deposition and characterization of Zn-Fe alloy^[7-9].

The electrodeposition of Zn-Fe alloys is classified by Brenner^[10] as an anomalous codeposition where zinc the less noble metal, deposits preferably with respect to the more noble iron. The reports show that the electrodeposition of Zn-Fe alloy in aqueous is classified as anomalous codeposition because the presence of zinc inhibits the electrodeposition of the more noble metal iron and the less noble zinc is preferentially deposited. As a result, the Zn/Fe ratio in the deposit is higher than in the electrolyte, and alloy deposits with high iron content are difficult to produce. Because of this, iron content in Zn-Fe alloys produced from aqueous plating baths is usually low. Due to such anomalous behavior, the codeposition of Zn-Fe in these solutions does not involve under potential deposition of Zn on Fe, although this phenomenon^[11] is known since 1907, the codeposition mechanisms of zinc and cobalt are not well understood^[12,13]. There are some propositions to explain the anomalous codeposition of the Zn-Fe alloys. The first attributes the anomalous codeposition to a local pH increase, which would induce zinc hydroxide precipitation and would inhibit the iron deposition^[14,15]. It was, however, later that anomalous codeposition occurred even at low current densities^[16], where hydrogen formation is unable to cause large alkalization effects. Another proposition is based on the under potential deposition of zinc on iron-rich zinc alloys or on iron nuclei^[17,18]. Matlosz used a two-step reaction mechanism involving adsorbed monovalent intermediate ions for both electrodeposition of iron and zinc, as single metals, and combines the two to develop a model for codeposition^[19]. Anomalous effects assumed to be caused by preferential Sasaki and Talbot^[20] proposed model extends the one-dimensional diffusion modeling of Grande and Talbot^[21] a supportive or interpretive, rather than a predictive, model of electrodeposition. A main contribution of this model is the inclusion of hydrogen adsorption and its effects on electrodeposition. Zech et. al. concluded that deposition of iron group metals leads to a reduction of the reaction rate of the more noble component and an increase of the reaction rate of the less noble component compared to single metal deposition^[22]. Eliaz and

Gileadi^[23] have recently reviewed the principles of alloy codeposition and the phenomenon of anomalous codeposition (ACD) in the frame work of a more comprehensive review of induced codeposition.

A good amount of serious work has already been documented pertaining to production and properties of Zn-M alloys with detailed mechanism of anomalous codeposition. It has also been shown that the corrosion resistance of Zn-M alloys is highly dependent on bath constituents and operating parameters employed for plating. Thus by proper modulation of $[Fe^{2+}]$, c.d. and temperature the corrosion resistance of Zn-Fe electroplates can be improved significantly. The present work illustrates the optimization of stable chloride bath for electrodeposition of Zn-Fe alloy over mild steel for its peak performance against corrosion.

EXPERIMENTAL

Plating solutions were prepared from reagent grade chemicals and distilled water. The composition of electrolytic bath was optimized by standard Hull cell method. All deposition was carried out 303K, except during temperature variation. The bath was maintained at pH 4.0 and monitored frequently. Polished mild steel panels having an exposed area of 7.5 cm² were used as cathode and pure zinc as anode with same exposed area. Mild steel panels were polished with emery paper (grit 600), degreased in an ultrasonic UM-2 bath, electro cleaned, treated with 10% HCl and then rinsed with distilled water before dipping into the electrolyte. Electroplating was carried out at different current density to study the effect of latter on deposit character. After deposition, the cathode was washed with tap water and rinsed with distilled water then dried. APVC cell of 250 cm³ capacity was used for electroplating with cathode-anode space of about 5cm. The corrosion behaviors of deposits were studied by d. c. and a. c. electrochemical techniques using Electrochemical Work Station (Metrohm PGSTAT 30) using three electrode system. The polarization measurements were made at 298K in aerated 5 % NaCl solution maintained at 6.0 pH. The saturated calomel electrode (SCE) was used as reference and pure platinum as counter. The potentiodynamic polarization was carried out at a scan rate of 1 mVs⁻¹. Potentiodynamic cyclic polarization was

carried out over the potential range of -1.6V to -0.4V at the scan rate of 1 mVs⁻¹ (Gamry Instruments) and impedance behavior of electroplates were studied by Nyquist plot in the frequency range from 10 MHz to 10 mHz. The composition of coatings was analyzed by colorimetric method by stripping the electrodeposits into dilute HCl^[24], and was cross verified with EDX analysis. The thickness of the deposits was calculated from Faraday's equation:

$$t = E \times I_c \times C.E. \times \Delta t / (d \cdot F)$$

Where t is the thickness of the deposit, E is an electrodeposit coating equivalent, I_c is a film deposition current density, C.E. is a current efficiency, Δt is a time interval, and d is the density of the deposit and F is Faradays constant (96,500 Coulombs). The validity of measured thickness was checked using digital thickness tester (Coat measure M&C, ISO-17025/2005). The hardness of the deposit (~15 μm thickness) was measured by Vickers method using Micro Hardness Meter (CLEMEX). The cathode current efficiency of deposition was determined by knowing the mass and composition of the deposit^[10]. The surface roughness of the deposit was found out by AFM. The surface morphology of electroplates were studied by Scanning Electron Microscopy (SEM, JEOL 6380 LA) with EDX link. X-ray Photoelectron Spectroscopy (XPS) measurements were performed in UHV (2.5x10⁻¹⁰ Torr base pressure) using 5600 Multi-Technique System (PHI, USA).

RESULTS AND DISCUSSIONS

Hull cell studies

Acid bath containing ZnCl₂, FeCl₂, sulphanilic acid, and gelatin has been optimized by conventional Hull cell method at 1A cell current, pH 4.0 and temperature 303K. Ascorbic acid was used to prevent the oxidation of Fe²⁺ to Fe³⁺. Varieties of deposits having grayish white/bright/semi-bright/porous/black powdery appearance were obtained over the wide c.d. of 1.0-5.0 A dm⁻². Effect of each bath constituents on Hull cell panels were examined in terms of their appearance, brightness and surface morphology. NH₄Cl and KCl were used as conducting salts for improving the homogeneity and brightness of the deposit. Bath constituents and operating parameters of the

optimized bath are given in TABLE 1.

TABLE 1 : Composition and operating parameter of optimized bath for electrodeposition of bright Zn-Fe alloy

Bath composition	Amount (M)	Operating parameters
Zinc chloride	0.37	pH : 4.0
Ferrous chloride	0.04	Temperature : 303 K
Ammonium chloride	2.24	Anode : Pure zinc
Potassium chloride	1.61	current density: 3.0 A dm ⁻²
Sulphanilic acid	0.03	
Gelatin	7g/lit	
Ascorbic acid	10g/lit	

Effect of current density

Wt. % Fe in the deposit

Factors which enhance the wt. % Fe in electrodeposited alloys were studied by varying c.d., pH, and temperature. The dependency of c.d. and pH of the bath on wt. % Fe, hardness, thickness and appearance of the deposit are shown in the TABLE 2. The bath produced semi-bright deposit with about 1.31 wt. % Fe at low c.d. and produces a grayish bright porous deposit at high c.d. with about 4.99 wt% Fe. A good deposit of Zn-Fe was found at 3.0 A dm⁻² with about 3.16 wt. % Fe. The increase of wt. % Fe in the deposit with c.d. is attributed to preferential deposition of Iron due to rapid depletion of Zn⁺² ions at cathode film.

TABLE 2 : Effect of current density and pH on wt. %Fe, hardness, thickness, CCE and deposit patterns of electroplates at 303K

Current density (A dm ⁻²)	pH of bath	Wt. %Fe in deposit	Vickers hardness V ₂₀₀	Thickness Of Deposit μm	CCE (%)	Appearance of deposit
1.0	4.0	1.31	145	5.15	93.26	Semi bright
2.0	4.0	2.18	171	10.47	92.10	Bright
3.0	4.0	3.16	175	15.08	91.43	Bright
4.0	4.0	3.79	177	19.90	90.57	Bright
5.0	4.0	4.99	189	24.20	88.27	Grayish bright
3.0	2.0	2.98	-	-	-	Semi bright
3.0	3.0	3.16	175	15.08	-	Bright
3.0	5.0	3.24	-	-	-	Bright

Thickness of deposit

The thickness of the deposit was found to increase with c. d. as shown in TABLE 2. The linear dependency of thickness of the deposit with c.d. as per the Faraday's equation, and also increase in the metal % in the deposit with the current density.

Full Paper

Hardness of deposit

The hardness of deposit was found to increase with wt. % Fe in the deposit as shown in TABLE 2. Increase in the wt % of Fe is observed with c. d. It may be ascribed by the inherent high density Iron ($d_{Zn} = 7.14 \text{ g cm}^{-3}$ and $d_{Fe} = 7.86 \text{ g cm}^{-3}$) in the deposit.

Effect of pH

Generally, during Zn-Fe group metal alloy deposition there will be a small change in pH after plating if the bath contains simple metallic ions. But in the bath under study, there was a significant increase in the pH of the bath after plating at low pH and remained almost same at high pH. To understand the effect of pH on deposition patterns, the pH of the bath was varied from 2 to 5 and corresponding data are given in TABLE 2. At low pH, the deposit was semi-bright and powdery and no much change in the appearance of the deposit was found at high pH. Increase of wt. % Fe in the deposit with pH indicates that the metal ions are in complex form due to additive (sulphanilic acid with NH_4^+ ions).

Effect of Temperature

Temperature has prominent role on the composition and appearance of the deposit as exhibited by other Zn-M alloys. The deposit was found to be grayish white at high temperature with more iron compared to semi bright at low temperature with less wt.% Fe. The variation of wt. % Fe with temperature is as shown in TABLE 3. At elevated temperature, more readily depositable metal (zinc) ions are favored to be replenished fast at the cathode and hence decrease the iron content in the alloy was found.

TABLE 3 : Effect of temperature on wt. %Fe in the deposit at 3.0 Adm² and pH 4.0

Temp. (K)	wt. %Fe in the deposit	Appearance of the deposit
283	4.17	Semi Bright
293	3.94	Bright
303	3.16	Bright
313	3.08	Bright
323	3.00	Grayish white

Cathode current efficiency (CCE)

Cathode current efficiency is given by,

$$\% \text{ Current efficiency} = \frac{\text{Weight of the alloy deposited} \times 100}{\text{Theoretical weight obtained from Faraday's laws}}$$

$$= \frac{M \times 100}{e_{\text{alloy}} \times Q}$$

Where M is the mass of the alloy deposit, Q is the quantity of the electricity passed and e_{alloy} is the electrochemical equivalent. The CCE of the bath remains almost constant at low c.d. and was found to decrease slightly at high c.d. due to hydrogen evolution at the cathode as shown in TABLE 2.

Corrosion study

Tafel plots

Corrosion resistance of Zn-Fe electroplates were determined using 5% NaCl solution by Tafel's extrapolation method and data are given in the TABLE 4. Polarization studies have been made at a scan rate of 1 mV/s in a potential ramp of +0.5V cathodic and -1.0V anodic from open circuit potential (OCP) as shown in Figure 1. The anodic polarization was studied up to -1.0V from OCP to check the possibility of passive film formation which is likely to inhibit the corrosion under certain conditions of applied potential.

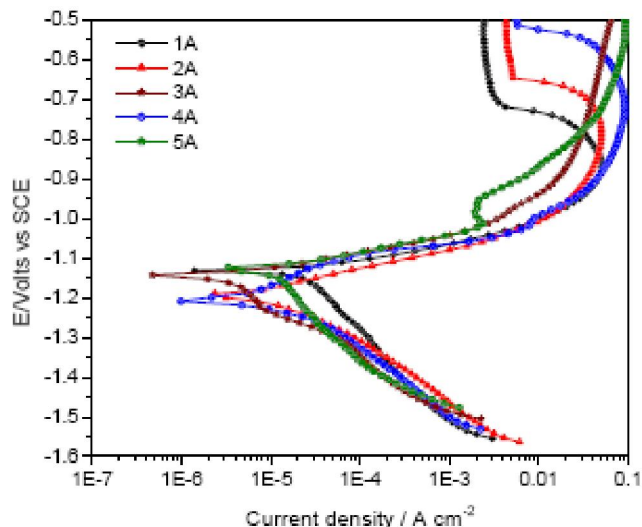


Figure 1 : Tafel plots for Zn-Fe alloy deposits obtained at different c.d.'s from the optimized bath at scan rate of 1 mV/sec vs. SCE

E_{cor} and Tafel's slopes for electroplates at different c.d.'s are shown in TABLE 4. Tafel slope indicates that

the corrosion of Zn-Fe electroplates are cathodic controlled and deposit at 3.0 Adm^{-2} is found to be very smooth and uniform with peak performance against corrosion.

TABLE 4 : Corrosion properties of Zn-Fe alloy deposits obtained under different current densities using 5% NaCl at 301K

Current density (A dm^{-2})	Wt. % Fe in deposit	E_{corr} in Volts Vs. SCE	β_a (V/dec)	β_c (V/dec)	i_{corr} ($\mu\text{A. cm}^{-2}$)	Corrosion rate (mm y^{-1})
1.0	1.31	-1.134	0.083	0.233	38.80	0.559
2.0	2.18	-1.164	0.085	0.163	26.39	0.380
3.0	3.16	-1.144	0.088	0.165	22.58	0.325
4.0	3.79	-1.231	0.146	0.167	28.71	0.414
5.0	4.99	-1.127	0.179	0.190	34.88	0.502

Cyclic potentiodynamic polarization (CPP) measurements

The peak corrosion resistance exhibited by Zn-Fe coating may be better understood by investigating the CPP study over a potential range of -1.6V to -0.2V as shown in Figure 2. In the range of -0.2 to -0.60V , the current density of backward scanning is higher than of the forward scanning, indicating that the dissolving of oxides had occurred in the process of forward scanning, so self-repairing occurred in the process of backward scanning and the increased anodic current appeared. In the range of -0.65 to -0.95V , current density of backward scanning was lower than that of forward scanning, which shows that metal could form pro-

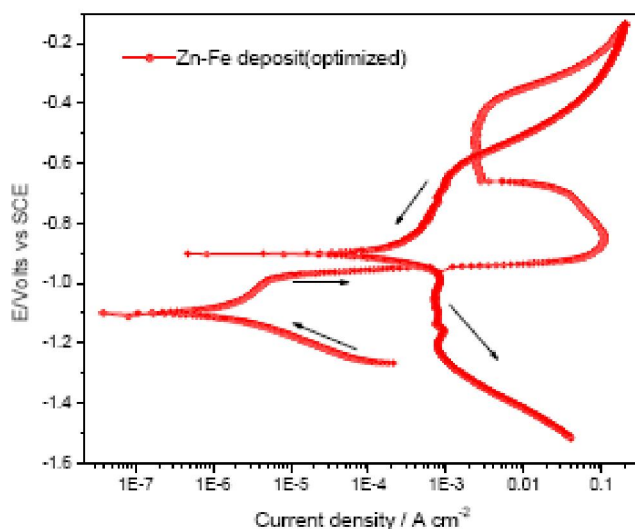


Figure 2 : Potentiodynamic cyclic polarization curve for Zn-Fe alloy deposit obtained at optimized current density of 3.0 Adm^{-2} from optimized bath at scan rate of 1 mV/sec vs. SCE

TECTIVE passivation film when the potential falls down to a certain value. But current density of backward scanning was lower than forward scanning at the same potential, which indicated that the passivation film had a more compact structure after been anodic polarized. The constancy of current density towards higher potential during forward scanning clearly indicates the formation of passive film.

Electrochemical impedance spectroscopy (EIS)

Electrochemical Impedance Spectroscopy (EIS) is a very versatile electrochemical tool to characterize intrinsic electrical properties of any material and its interface. The basis of EIS is the analysis of the impedance (resistance of alternating current) of the observed system in subject to the applied frequency and exciting signal. This analysis provides quantitative information about the conductance, the dielectric coefficient, the static properties of the interfaces of a system, and its dynamic change due to adsorption or charge-transfer-phenomena. EIS uses alternating current with low amplitude. This facilitates a non-invasive observation of any sample without any or less influence on the electrochemical state. Nyquist responses of Zn-Fe alloy deposits under different conditions of c.d. were shown in Figure 3. The solution resistance remains the same for all deposits since the studies were done under similar conditions. The capacitive loop with bigger semicircle indicates that the Zn-Fe deposit at 3.0 Amp/dm^2 (optimized c.d.) shows maximum polarization resistance (R_p).

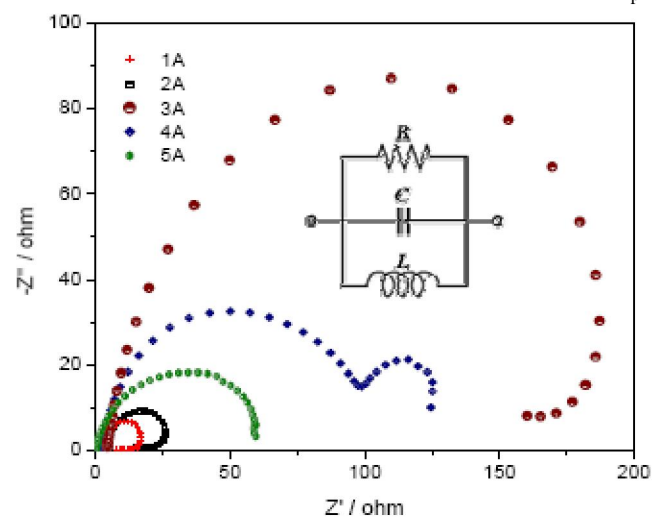


Figure 3 : Electrochemical impedance spectroscopic curves of Zn-Fe alloy coatings produced at different current densities from optimized bath with ECE (inset)

Full Paper

The increase and then decrease of imaginary component of impedance (Z'') with frequency indicates that resistance (R), capacitance (C) and inductance (L) of electrochemical circuit are in parallel combination its electrochemical equivalent circuit (EEC) is as shown in the Figure 3 (inset). The increased corrosion resistance of Zn-Fe alloy at optimized bath condition (3.0 A dm^{-2}) may be attributed to the increased reactance caused by the formation of semiconductor film at the interface.

Mott-schottky plot of Zn-Fe alloy coatings

Increased of corrosion resistance of coatings at optimized bath condition may be attributed to the formation of semiconductor film at the interface of metal and the medium during corrosion. The semiconductor property of the passivation film can be described with Mott-Schottky equation.

$$\text{n-type} : \frac{1}{C^2} = \frac{2}{e \epsilon_0 e N_D} \left(E - E_{fb} - \frac{kT}{e} \right)$$

$$\text{p-type} : \frac{1}{C^2} = - \frac{2}{e \epsilon_0 e N_A} \left(E - E_{fb} - \frac{kT}{e} \right)$$

where C is the capacitance of space charge layer of the passive film, E the given potential, ϵ the dielectric constant of the passivation film, ϵ_0 the vacuum dielectric constant, e the electronic quantity, N_D and N_A stand for the donor and acceptor electron density, E_{fb} is the flat band potential, k the Boltzmann constant, T the absolute temperature.

When adopted Eq (1) and Eq(2) to describe the electronic property of metal surface passivation film, the key point is to determine the capacitance of the space charge layer, and the space charge amount of the passivation film is related to the capacitance measured from experiment. Therefore, when the range of the given potential changed widely, the space charge amount of the passivation film may change largely, it should be divided to different potential during the analysis. The type of semiconductor can be determined from the $1/C^2$ versus E plot. Figure 4 shows the C^{-2} versus E profile for Zn-Fe coating at optimized processing parameter is a linear plot with positive slope, indicates that n-

type semiconductor film formed during corrosion is responsible for its improved resistance.

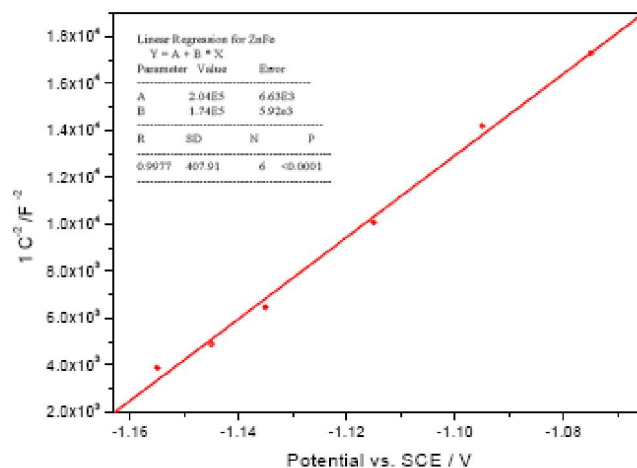


Figure 4 : Mott-schottky plot showing n-type semiconductor behavior of ternary Zn-Fe alloy deposit obtained from optimized current density

X-ray fluorescence spectral (XPS) study

The samples were irradiated with an Al $K\alpha$ monochromated source (1486.6 eV) and the outcome electrons were analyzed by a Spherical Capacitor Analyzer using the slit aperture of 0.8 mm. The samples were analyzed at the surface and after sputter cleaning with 4 kV Ar^+ ion gun (sputter rate was $\sim 43 \text{ A/min}$ on the reference SiO_2/Si sample). All the samples were charged at the surface, before sputter cleaning. Neutralizer was used for charge compensation. Additional mathematical shift was used when necessary, to reference all the peaks to C_{1s} at 285 eV.

XPS and surface etching by ionized argon were applied to analyze the metals within the corrosion product layer (Figure 5). The discrimination of Zn and ZnO are not possible as the Zn 2p $_{3/2}$ spectra are similar for both the non-oxidized and the oxidized metals (1021.6 eV and 1021.7 eV, respectively). To solve this problem, Auger spectrum of Zn(L3M45M45) was recorded (the kinetic energy for Zn is 992.3 eV, while the energy for ZnO is 987.6 eV). According to the electron energy peaks, iron was found within the outer layer in the non oxidized form, while zinc was in the oxidized one. Figure (6a). After sputtering in deeper levels, Zn appears as indicated by the energy peak at 992 eV (Figure 6b). Iron, however, was found to be non-oxidized within the con-

centration profile studied. This result implies that the corrosion of zinc, as a less noble component, is pre-

vailing during the first corrosion stages, whereas more noble iron remains non-corroded.

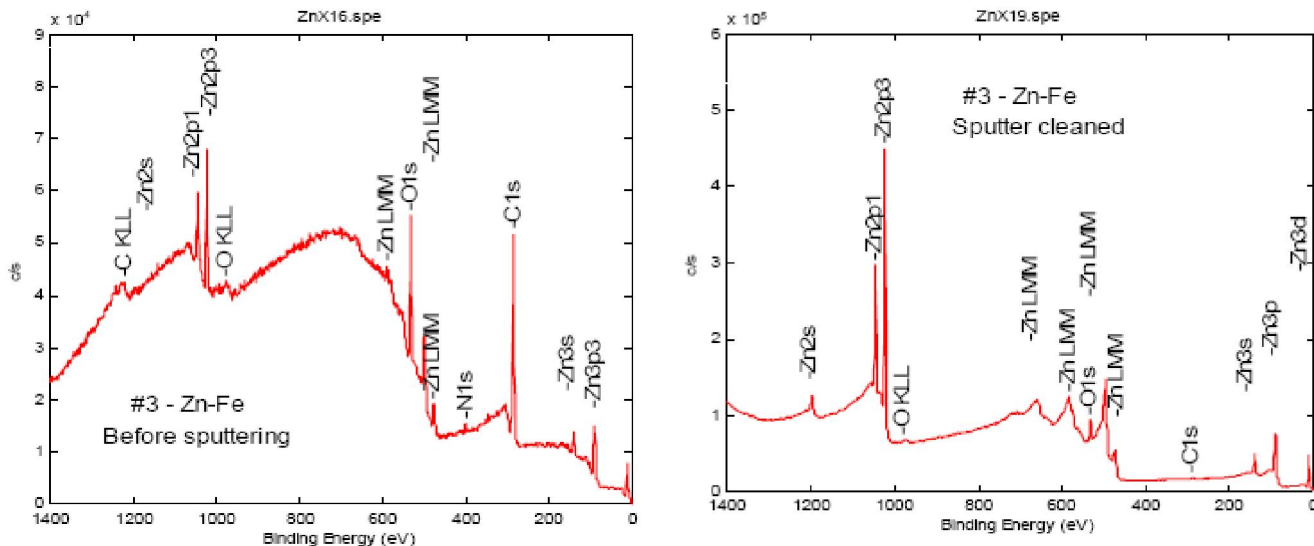


Figure 5: X-ray fluorescence spectroscopic curves of Zn-Fe alloy coatings at the optimized current density 3.0 A dm^{-2} before and after sputtering

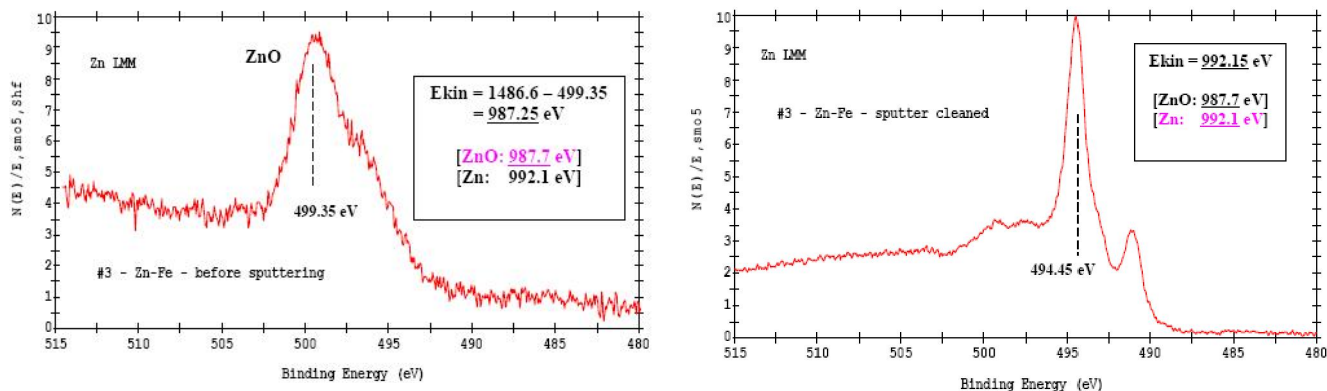


Figure 6: X-ray fluorescence spectroscopic curves of Zn_{LMM} peak of Zn-Fe alloy deposits at optimized current density of 3.0 A dm^{-2} before after sputtering

Surface study

The AFM study revealed that the surface roughness of the deposit were in the order of $\sim 10\text{-}80 \text{ nm}$ (Figure 7). The photomicrograph of the showed that c.d. plays a significant role on the phase structure of the deposit. The variation in the surface morphology of the deposit with c.d. is shown in Figure 8. It was found that surface homogeneity increase with c.d. as shown in Figures 8a and 8b. At optimized c.d. of 3.0 A dm^{-2} the granular uniform structure was observed. At high c.d. 4.0 A dm^{-2} thick and porous deposits was found (Figure 8d). The composition of the Zn-Fe alloy coatings obtained from the optimized bath was confirmed by EDX analysis

as shown in Figure 9.

CONCLUSIONS

A stable bath for electroplating of bright Zn-Fe alloy over mild steel has been proposed. Under conditions of investigations, the bath followed anomalous codeposition with preferential deposition of Zinc. The temperature on the plating process showed that the codeposition of metals is diffusion controlled. The corrosion resistance of electroplates were not direct function of its wt. % Fe but also surface morphology. The electrodeposits having about 3.16 wt. % Fe was found

Full Paper

to be very smooth and uniform showing good performance against corrosion. The XPS study implies that the corrosion of zinc, as a less noble component, is prevailing during the first corrosion stages, whereas more noble cobalt remains non-corroded. The use of the sulphanic acid has significant role in improving homogeneity and grain size of the deposit. AFM study showed that the surface roughness of the deposit ob-

tained at optimized c.d. is of the order of 10-80 nm. CPP study confirmed that the formation of passive film, responsible for improved corrosion resistance of coatings. The thickness and porosity of deposits increased with current density. EIS study revealed that superior corrosion resistance of Zn-Fe coatings is due to n-type semiconductor film at the interface, as evidenced by the M-S plots.

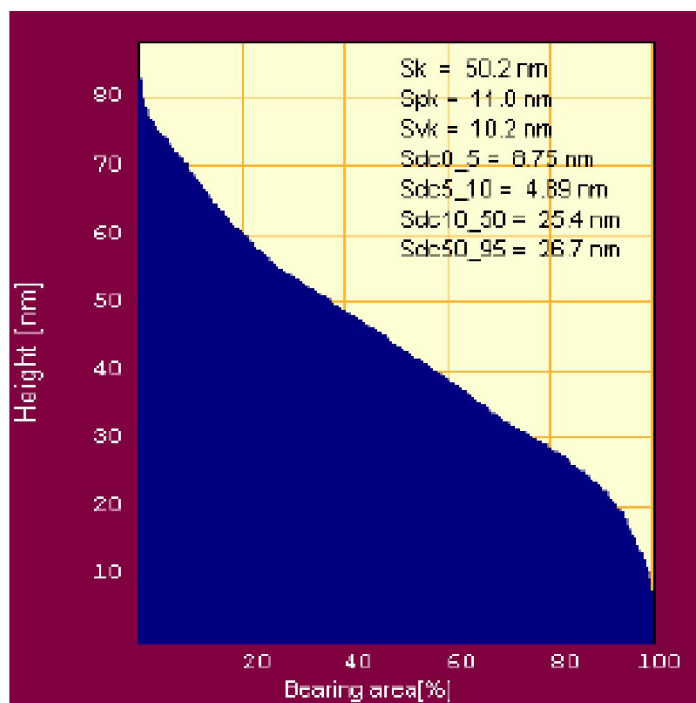
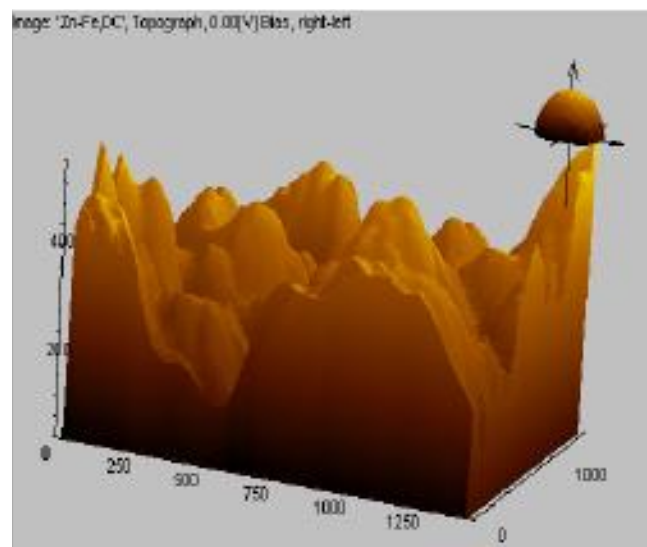
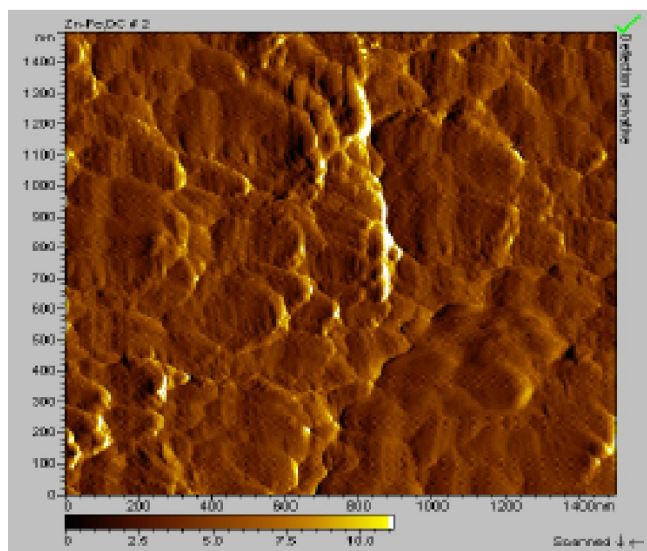


Figure 7 : AFM micrographs and surface roughness of Zn-Fe alloy deposit produced at optimised current density of 3.0 A dm^{-2} from optimised bath

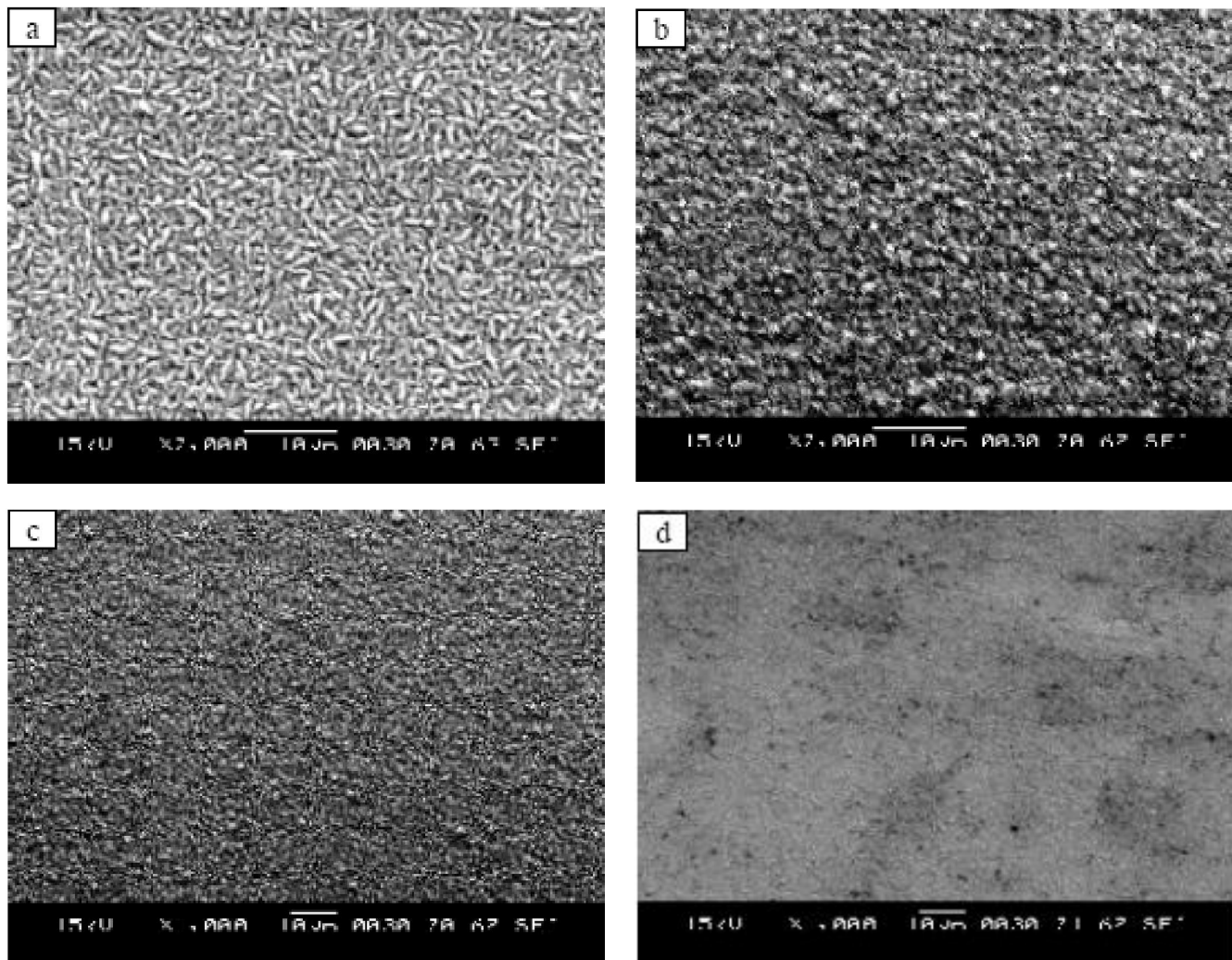


Figure 8 : SEM micrographs of Zn-Fe alloy deposit produced at different current densities (a) 1.0 A dm⁻², (b) 2.0 A dm⁻²(c) 3.0A dm⁻²(d) 4.0A dm⁻²from the optimised bath

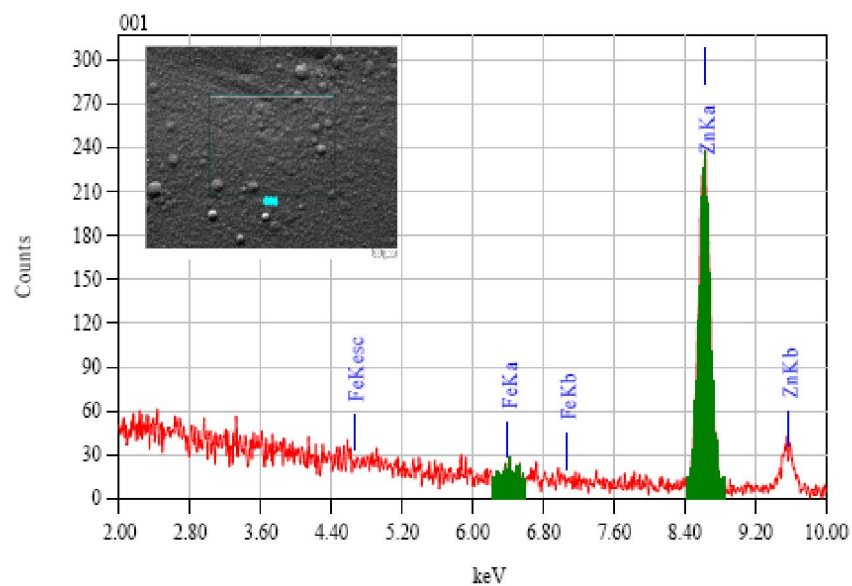


Figure 9 : EDX diagram of Zn-Fe alloy at the optimized current density of 3.0 A dm⁻²from optimized bath

REFERENCES

- [1] D.E.Hall; *Plat.Surf.Finish.*, **70**, 59 (1983).
- [2] R.Fratesi, G.Roventi, G.Giuliani; *J.Appl.Electrochem.*, **27**, 1088 (1997).
- [3] Jelena B.Bajat, Miskovic-Stankovic, V.B.Kacarevic-Popovic; *Prog.Org.Coat.*, **47**, 49 (2003).
- [4] C.J.Lan, W.Y.Liu, S.T.Ke, T.S.Chin; *Surf.Coat.Technol.*, **201**, 3103 (2006).
- [5] Jelena B.Bajat, B.Vesna, Miskovic-Stankovic, Miodrag D.Maksimovic, Dagutin M.Drazic; *Slavica Zec:J.Serb.Chem.Soc*, **69(10)**, 807 (2004).
- [6] A.M.Alfantazi, U.Erb; *Corro.Eng.*, **52**, 880 (1996).
- [7] M.Gladkovas, V.Burokas, A.Martusiene, D.Bucinskiene; *Chemija*, **T.12, Nr.2**, 114 (2001).
- [8] F.Y.Ge, S.K.Xu, S.B.Yao, S.M.Zhou; *Surf.Coat.Technol.*, **88**, 1 (1996).
- [9] Z.N.Yang, Z.Zhang, J.Q.Zhang; *Surf.Coat.Technol.*, **200**, 4810 (2006).
- [10] A.Brenner; 'Electrodeposition of alloys', Academic Press New York, **2**, (1963).
- [11] E.P.Shoch, A.Hirsch; *J.Am.Chem.Soc.*, **29**, 314 (1907).
- [12] M.F.Mathias, T.W.Chapman; *J.Electrochem.Soc.*, **137**, 102 (1990).
- [13] S.Swathirajan; *J.Electroanal.Chem.*, **221**, 211 (1987).
- [14] E.Gomez, E.Pelaez, E.Valles; *J.Electroanal.Chem.*, **469**, 139 (1999).
- [15] K.Higashi, H.Fukushima, V.Takayushi, T.Adaniya, K.Matsudo; *J.Electrochem Soc.*, **128**, 2091 (1981).
- [16] J.Horans; *J.Electrochem Soc.*, **128**, 45 (1981).
- [17] M.J.Nicol, H.I.Philip; *J.Electroanal.Chem.*, **70**, 233 (1976).
- [18] S.Swathirajan; *J.Electrochem Soc.*, **133**, 671 (1986).
- [19] M.Matlosz; *J.Electrochem Soc.*, **140**, 2272 (1993).
- [20] Y.Keith Sasaki, J.B.Talbot; *J.Electrochem Soc.*, **147**, 189 (2000).
- [21] W.C.Grande, J.B.Talbot; *J.Electrochem Soc.*, **140**, 67 (1993).
- [22] N.Zech, E.J.Poldlaha, D.Landolt; *J.Electrochem Soc.*, **146**, 2886 (1999).
- [23] N.Eliasz, E.Gileadi C.G.Vayenas, R.E.White, M.E.Gamboa-Aldeco; 'Modern aspects of electrochemistry', **42**, Springer, New York, 191–301 (2008).
- [24] I.Vogel; 'Quantitative Inorganic Analysis', Longmans Green and Co, London, 195.
- [25] U.Stimming; *Electrochim Acta*, **31**, 415 (1986).
- [26] E.Sikora, D.Macdonald; *Electrochim Acta*, **48**, 69 (2002).